Preparation and characterization of zinc sulfide thin film deposited on quartz substrate from sintered targets by electron beam evaporation

YANWEI HUANG[*], LEFAN XIAO, XUELI LIU, JUNHUA XI, ZHENGUO JI
College of Materials and Environmental Engineering, Hangzhou Dianzi University, Hangzhou 310018, China

Zinc sulfide thin films were deposited on quartz substrate from sintering targets by electron beam evaporation. The structural, morphological and optical properties of the films were investigated by X-ray diffraction (XRD), scanning electron microscopy (SEM), photoluminescence and UV-vis spectra. XRD analysis indicated that prepared ZnS thin film showed hexagonal polycrystalline wurtzite structure with (110) preferential direction. The structure of films has the accordance with sintered targets by electron beam evaporation. SEM images revealed the films were constituted of nanoparticles with diameter of several dozens of nanometers or even smaller, which has been vertified by calculated result of grain size. The photoluminescence spectra showed the emission peak was located at 370 nm with excitation wavelength of 250 nm, which may be caused by donor-acceptor band transition. From the transmission spectra, the thickness and optical band gap have been calculated and fitted, and the result indicated the film has broader optical band gap, about 3.75 eV.

1. Introduction

As one kind of outstanding semiconductor, ZnS has been widely used in optoelectronic devices because of its wide and direct band gap (about 3.8 eV), good fluorescence and electroluminescence properties. ZnS thin film is also a promising buffer layer material in $Cu(In,Ga)Se_2(CIGS)$-based or $Cu_2ZnSnS_4(CZTS)$-based solar cell. Although the buffer layer of high-efficiency CIGS solar cells, with the highest efficiency of 20%, is usually CdS thin film deposited by chemical bath deposition [1], Cd causes serious environmental problems due to plenty of Cd compound waste during the mass manufacturing of solar cells. In addition, the band gap of CdS is narrow, about 2.42 eV, which causes the drop of quantum efficiency in the shorter wavelength region. As a result, Cd-free buffer layers with broad band gap should be developed. ZnS thin film has been considered as a potential alternative buffer layer in CIGS-based solar cells because it is less toxic and cheap. Furthermore, the wider band gap of ZnS make it possible to be transparent to almost all wavelengths of the solar spectrum [2], which benefits improvement of short-circuit current of cells. Meanwhile, ZnS can also reduce the band offset of the ZnS/ZnO layer because its band gap is close to the ZnO band gap (3.4 eV). Recently, some groups have reported high-efficiency CIGS devices where the CdS buffer layer is replaced by ZnS layer [3].

ZnS thin film buffer layers have been prepared by various methods such as sputtering [4,5], molecular beam epitaxy (MBE) [2], chemical vapor deposition [6], chemical bath deposition (CBD) [7,8], electro-deposition [9] spin coating [10]. Among these methods, CBD method has been widely used to synthesize CdS or ZnS buffer layer in CIGS thin film solar cells. Although CBD method has some advantages such as convenient, simple and inexpensive, ZnS thin film by CBD method contained a large amount of oxygen element in the form of Zn-O and Zn-OH bonds due to the basic aqueous alkaline solution used to grow the ZnS films [11, 12]. Besides, CBD method belongs to a kind of wet solution method from where the synthesized film is susceptible to sputtering damage in the following growth of CIGS absorber and ZnO window layer process. Electron beam evaporation (EBV) has some advantages over the other methods, such as low cost, high power, and environment-friendly, especially in ablating those materials with high-melting-point. In the present work authors have synthesized wurtzite-structured ZnS thin films on quartz substrate from sintering disc targets by electron beam evaporation, and have investigated the structural, morphological and optical properties of films. The photoluminescence and transmission spectra were measured and analysized. Through the theoretical fitting of optical curves, the films thickness and optical band gap were obtained.

2. Experimental details

Powder of zinc sulfide (Alfa Aesar, 99.9%) was pressed at 5 MPa into some small discs with diameter of

13 mm and thickness of 1.5 mm. These discs were sintered at 800℃ or 1000℃ for 12 h in nitrogen ambience protection and then ceramic-like ZnS targets were obtained. The prepared ZnS targets possess wurtzite structure. For the electron beam evaporation, the crucible should be filled with source material, ZnS targets. Prior to deposition, the vacuum chamber was evacuated to the base pressure of 5.0×10^{-4}Pa and the quartz substrates were cleaned in alcohol and de-ionized water for 20 min in an ultrasonic bath, respectively. ZnS thin films were then deposited by electron beam evaporation from the targets in crucible. The high voltage is fixed at 6 kV, and the scanning current is 0.5 mA in X axis, 0 mA in Y axis, with the current fluctuation of ±0.05 mA. During the evaporation, electron beam current is fixed at 50 mA, the working pressure is 3.0×10^{-3}Pa. The ZnS thin films were deposited at room temperature for 50 min. The as-deposited film is a little yellowish, and when annealed at 400℃ in nitrogen atmosphere for 2 h, the color of films becomes heavier.

The phase structure and surface morphology were characterized by a X-ray diffraction photometer using Cu Kα (λ=0.15406 nm) radiation, a Field Emission Scanning Electron Microscopy (FE-SEM, FEI Quanta 450). Photoluminescence spectra were obtained in the spectrometry (RF-530 TPC, Shimadzu, Japan). The optical properties of the films were measured at normal incidence in the wavelength range from 320 to 800 nm using UV-vis spectrometry (UV-3600, Shimadzu, Japan).

3. Results and discussion

In Fig. 1, X-ray diffraction patterns are presented for ZnS targets sintered at 800℃ and 1000℃, respectively. The diffraction peaks identified in the targets were found to be consistent with the diffraction planes of hexagonal wurtzite structure of ZnS, agreeing with the PDF file no. 36-1450. When the sintering temperature increases from 800℃ to 1000℃, the peak intensity corresponding to same 2θ value changed distinctly. The ZnS target sintered at 1000 ℃ has been found to exhibit a preferred orientation along certain crystallographic planes which have been identified as (002), (110) and (112) planes respectively, of which the intensity of the (002) orientation is predominant. However, for the target sintered at 800℃ the diffraction peak intensity is located at the (101) orientation. The peaks marked with star at 2θ equal to 43.6° (800℃) and 33.1° (1000℃) were found to accord with the plane (440) and (200) of cubic ZnS (PDF file no. 05-0566), respectively, indicating that prepared targets belongs to polycrystalline structure with principal wurtize phase containing small cubic phase of ZnS. Besides, temperature increasing could effectively restrain the growth of (440) plane of cubic ZnS and while promote the growth of (200) plane of cubic ZnS.
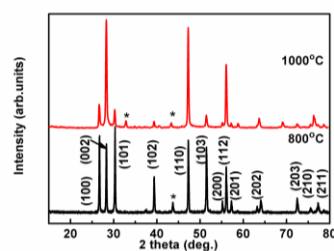
Fig. 1. X-ray diffraction patterns of ZnS targets sintered at 800℃ and 1000℃

X-ray diffraction patterns in Fig. 2 were shown for the ZnS thin films deposited by electron beam evaporation from the target sintered at 1000℃. As can be seen in Fig. 2 the film prepared at room temperature did not reveal any diffraction peak except a hump at 25°, which was due to substrate contribution. This indicated that ZnS thin film belongs to an amorphous structure. To improve the crystalline of film, ZnS films underwent a heat treatment process. However, ZnS could not be annealed in air because the oxygen accompanying with the moisture could accelerate oxidation process of ZnS. Here, as-prepared ZnS films were heated at 400℃ with the protection of nitrogen ambience from start to finish. The ZnS film annealed at 400 ℃ demonstrated a polycrystalline structure with (002), (110) and (112) planes consistent to the wurtize phase (PDF file no. 36-1450). Moreover, comparing the XRD patterns of target and prepared film, the predominant peaks (002), (110) and (112) in ZnS target sintered at 1000℃ have been inherited by the annealed ZnS film, revealing the trait of structure uniform from target to film by electron beam evaporation technology. L. X. Shao et al.[4] deposited ZnS thin films by RF reactive sputtering for photovoltaic applications, and they think that the wurtzite (002) peak at 28.5° in XRD patterns of ZnS possesses the almost same plane spacing with $CuInS_2$ absorber of the CIS based solar cells. Thus, ZnS fims prepared by this experiment could be an appropriate buffer layer deposited on absorber in CIGS-based solar cells. The crystallite size was estimated from the XRD results using Scherrer's formula (1):

$$D = \frac{0.89\lambda}{\beta\cos\theta}$$

(1)

Where β is the full width half maximum (FWHM) in radians and λ is the X-ray wavelength. Considering the (002), (110) and (112) planes, which are clearly visualized peaks in Fig. 1 and Fig. 2, the calculated values of grain size are summarized in Table 1. As it can be seen in Table 1, the deposited ZnS films have smaller grain size than that of ZnS targets, and the average size is about 13 nm. Fig. 3 shows surface morphology of ZnS thin film annealed at 400℃. From the image, it can be seen that the film has relatively uniform and compact surface structure and the ZnS film is composed of many crystalline grains with about several dozens of nanometers or even smaller. This can be conformed by calculated result of grain size in Table 1.

Table 1. Evaluation of crystallite size (nm) from the X-ray diffraction data.

Sample	Plane(002)	Plane(110)	Plane(112)	Average size
ZnS target(800℃)	33.138	35.104	36.454	34.899
ZnS target(1000℃)	23.838	35.102	36.453	31.789
ZnS film(400℃)	17.548	11.578	10.490	13.208
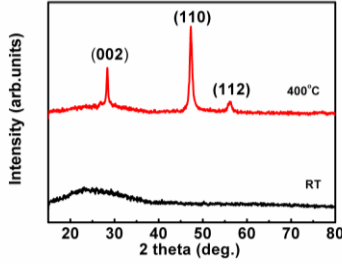
Fig. 2. X-ray diffraction patterns of ZnS thin films deposited by electron beam evaporation.
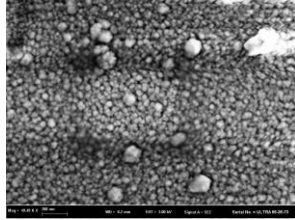
Fig. 3. SEM images of ZnS thin film annealed at 400℃

Fig. 4 shows the room-temperature PL spectra of the prepared ZnS films at the excitation wavelength of 250 nm. The insert shows the exciting light spectra. Both the samples show a typical violet emission located at around 370 nm. Commonly, the PL spectrum of ZnS film would trend to present a peak around 285 nm, which is due to the band edge emission [13]. In this paper, the band edge emission did not appear, but a broad peak around 370 nm could be clearly observed.
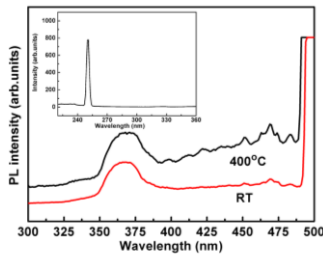
Fig. 4. Photoluminescence emission spectra of ZnS films prepared at room temperature and annealed at 400℃, respectively. The inset image shows the excitation spectra.

The peaks at longer wavelength can be attributed to native defects such as sulfur vacancies, zinc vacancies and interknots zinc. S. R. Chalana et al. [14] observed the emission peak located at 395 nm for ZnS film deposited by pulsed laser ablating, which was ascribed to the zinc

vacancies, and the peak at 411 nm can be due to the recombination between the sulfur-vacancy-related donor and the valence band. Y. Bouznit et al. reported their prepared ZnS thin films on glass substrates and also observed the emission peak at 396 nm [15]. Other similar results have been reported in previous studies for ZnS thin films or nanoparticles. Although there are no more evidence to explain the emission peak at 375 nm excited by 250 nm, we are apt to think that it was due to donor-acceptor band transition where some excess Zn acts as donor and some impurity or defects present at the surface and interface of the film acts as acceptor [16].

Fig. 5 shows the optical transmission spectra of ZnS films and the envelope lines of intensity maximum T_M and minimum T_m for ZnS films deposited at room temperature and annealed at 400 ℃. The average visible light transmission between 400 ~ 700 nm for the samples together with substrates is 62% and 45% for films deposited at room temperature and annealed at 400℃, respectively. The low visible light transmission can be ascribed to the thicker films, at the large growth rate by electron beam evaporation. The ZnS film thickness can be calculated from the following expressions (2), (3), (4) [17]:

$$n = [N + (N^2 - s^2)^{1/2}]^{1/2} \tag{2}$$

$$N = 2s \frac{T_M - T_m}{T_M T_m} + \frac{s^2 + 1}{2} \tag{3}$$

$$d = \frac{\lambda_1 \lambda_2}{2(\lambda_1 n_2 - \lambda_2 n_1)} \tag{4}$$

Where s is the refractive index of the quartz substrate, and, n_1 and n_2 are the refractive indices at two adjacent maxima (or minima) at the wavelengths λ_1 and λ_2. The value of d, that is, the film thickness can be roughly inferred from the above formulas. And the calculated ZnS films is about 3 ~ 5 μm. The thicker film can give rise to strong absorption, decreasing the optical transmission. The optical band gap (E_{og}) can be determined by the absorption coefficient (α) and photon energy ($h\nu$) as follows (5) [18]:

$$\alpha = \frac{B(h\nu - E_{og})^n}{h\nu} \tag{5}$$

Where B is a constant and the exponent n could have the values of 1/2, 3/2, 2 and 3, depending on the type of the electronic transition in *k*-space. For the allowed direct interband transition in a crystal, the best fit of $\alpha h\nu$ as a function of $h\nu$ is obtained with n=0.5. The values of E_{og} can be obtained by extrapolations of the linear regions of the plots to zero absorption. Fig. 6 and Fig. 7 shows the relationship between $(\alpha h\nu)^2$ and $h\nu$ for ZnS films prepared at room temperature and annealed at 400℃, corresponding to the amorphous structure and polycrystalline structure, respectively. The direct band gap of ZnS thin films annealed at 400℃, as found in the Fig.6 is 3.75 eV, which is very close to the theory value of ZnS bulk material. With this broad band gap, ZnS film is very suitable for application in CIGS solar cells as buffer layer between

absorption layer and window layer. Usually, the window layer is ZnO film deposited by sputtering or other vacuum method, whose band gap matches well with that of ZnS film. Thus, ZnS buffer layer can broaden the range of spectral response in short wavelength area. Besides, the electron beam evaporation method is compatible with other vacuum methods. From Fig. 7, the determined band gap for ZnS amorphous structure is 3.6 eV, which is smaller than that of polycrystalline structure. This is due to the band tail extending to the energy gap in amorphous semiconductors, which is consistent to our previous reported for other semiconductor oxide materials [19, 20].
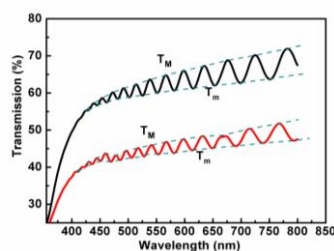
Fig. 5. Optical transmission spectra of ZnS thin films and the envelope lines of intensity maximum T_M and minimum T_m.
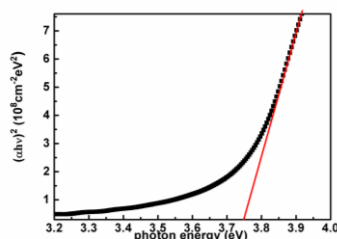
Fig. 6. $(\alpha h\nu)^2$ versus $h\nu$ curves for ZnS film annealed at $400\,^{\circ}\!C$
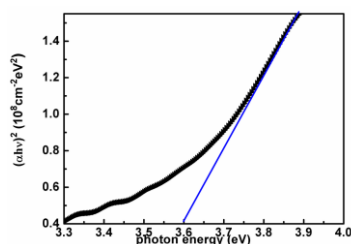
Fig. 7. $(\alpha h\nu)^2$ versus $h\nu$ curves for ZnS film deposited at room temperature.

4. Conclusions

The ZnS thin films with polycrystalline wurtzite structure were deposited on quartz substrate from sintering targets by electron beam evaporation. The structural, morphological and optical properties of the films were investigated by X-ray diffraction (XRD), scanning electron microscopy (SEM), photoluminescence and UV-vis spectra. The properties of ZnS thin film with polycrystalline and amorphous structure are investigated in comparison. The films annealed at $400\,^{\circ}\!C$ demonstrated were constituted of nanoparticles with diameter of several dozens of nanometers. The transmission spectra and photoluminescence revealed the films have broader optical band gap and violet emission peak. That is appropriate to use prepared ZnS thin film as buffer layer in CIGS solar cell to broaden light response range in short wavelength.

References

[1] I. Repinsl, B. Contreras, C. Egaas, J. Dehart, C. Scharf, B. Perkins, B. Noufi, Res. Appl. **16**, 235 (2008).
[2] M. M. Islam, S. Ishizuka, A. Yamada, K. Sakurai, S. Niki, T. Sakurai, K. Akimoto, Solar Energy Materials & Solar cells **93**, 970 (2009).
[3] A. Ennaoui, Renew. Energy **49**, 68 (2013).
[4] Le-Xi Shao, Kuen-Huei Chang, Huey-Liang Hwang, Applied Surface Science **212-213**, 305 (2003).
[5] V. L. Gayou, B. Salazar-Hernandez, M. E. Constantino, E. R. Andre's, T. Di'az, R. D. Macuil, M. R. Lo'pez, Vacuum, **84**, 1191 (2010).
[6] Zhao Yang Zhong, Eou Sik Cho, Sang Jik Kwon, Materials Chemistry and Physics **135**, 287 (2012).
[7] A. Goudarzi, G. M. Aval, R. Sahraei, H. Ahmadpoor, Thin Solid Films **516**, 4953 (2008).
[8] Seung Wook Shin, So Ra Kang, K. V. Gurav, Jae Ho Yun, Jong-Ha Moon, Jeong Yong Lee, Jin Hyeok Kim, Solar Energy **85**, 2903 (2011).
[9] A. Kassim, S. Nagalingam, H. S. Min, N. Karrim, Arabian J. Chem. **3**, 243 (2010).
[10] Yunfei Sun, Jinghai Yang, Lili Yang, Jian Cao, Ming Gao, Zhiqiang Zhang, Zhe Wang, Hang Song, Journal of Solid State Chemistry **200**, 258 (2013).
[11] D. H. Shin, J. H. Kim, S. T. Kim, L. Larin, E. A. Al-Ammar, B. T. Ahn, Sol. Energy Mat. Sol. C **116**, 76 (2013).
[12] Jun Liu, Aixiang Wei, Yu Zhao, Journal of Alloys and Compounds **588**, 228 (2014).
[13] N. Kumbhojkar, V. V. Nikesh, A. Kshirsagar, S. Mahamuni, J. Appl. Phys. **88**, 6260 (2000).
[14] S. R. Chalana, R. Vinodkumar, I. Navas, V. Ganesan, V. P. Mahadevan Pillai, Journal of Luminescence **132**, 944 (2012).
[15] Y. Bouznit, Y. Beggah, Mingsong Wang, N. Tabet, Journal of Luminescence **151**, 76 (2014).
[16] P. Roy, J. R. Ota. S. K. Srivastava, Thin Solid Films **515**, 1912 (2006).
[17] Martin Jerman, Zhaohui Qiao, Dieter Mergel, Applied Opt, **44**, 3006 (2005).
[18] J. Tauc, R. Grigorovid, A. Vancu, Phys. Status Solidi \ **15**, 627 (1966).
[19] Yanwei Huang, Qun Zhang, Guifeng Li, Ming Yang, Materials Characterization **60**, 415 (2009).
[20] Yanwei Huang, Guifeng Li, Jiahan Feng, Qun Zhang, Thin Solid Films **518**, 1892 (2010).

*Corresponding author: yanweihuang@gmail.com